© Universiti Tun Hussein Onn Malaysia Publisher's Office

IJIE

http://penerbit.uthm.edu.my/ojs/index.php/ijie
ISSN : 2229-838X e-ISSN : 2600-7916

The International Journal of Integrated Engineering

Assessment of Global Geopotential Models for Modelling Malaysia Marine Geoid

Noor Anim Zanariah Yahaya[1], Ami Hassan Md Din[1*], Abdullah Hisam Omar[1], Nazirah Mohamad Abdullah[2], Nornajihah Mohammad Yazid[1,3], Muhammad Faiz Pa'suya[4], Mohamad Ikbar Abdul Wahab[5]

[1]Faculty of Built Environment and Surveying,
Universiti Teknologi Malaysia, 81310 Johor Bahru, Johor, MALAYSIA

[2]Faculty of Applied Sciences and Technology,
Universiti Tun Hussein Onn Malaysia, Pagoh Higher Education Hub, 84600, Pagoh, Johor, MALAYSIA

[3]Department of Civil Engineering, Centre for Diploma Studies,
Universiti Tun Hussein Onn Malaysia, Pagoh Higher Education Hub, 84600, Pagoh, Johor, MALAYSIA

[4]Environment and Climate Change Reseach Group, Faculty of Architecture, Planning and Surveying,
Universiti Teknologi MARA, 02600 Arau, Perlis, MALAYSIA

[5]Quality Engineering Department,
Universiti Kuala Lumpur, Malaysian Institute of Industrial Technology, 81750 Johor Bahru, Johor, MALAYSIA

*Corresponding Author

DOI: https://doi.org/10.30880/ijie.2022.14.05.002
Received 21 February 2022; Accepted 01 July 2022; Available online 25 August 2022

Abstract: The evaluation towards global geopotential models represents a significant part in modelling the localised Marine Geoid. The marine geoid provides the vertical reference information in Marine Spatial Data Infrastructures (MSDI) development response to United Nations Sustainable Development Goals 14 for the sustainable development in marine environment. The main purpose of this study is to select the best model from both combined missions and satellite-only missions for the Malaysian region. The gravity anomaly field from 30 global models were exclusively calculated over the selected study area within 11 years period-time. Afterwards, each dataset was extracted from the ICGEM server to evaluate with the airborne-derived gravity anomaly from the Department of Surveying and Mapping, Malaysia. The internal accuracy, root mean square error (RMSE) and differences between every model and airborne data were computed. The result indicates GGM-derived gravity anomaly for the best combined mission is GECO with RMSE of 8.44 mGal and the standard deviation value of 28.034 mGal. While, the model from Gravity field and steady state Ocean Circulation Explorer (GOCE) namely, the GO_CONS_GCF_2_DIR_R5 is the best for the satellite-only mission with RMSE of 17.43 mGal and the standard deviation value of 22.828 mGal. As a conclusion, GECO model is preferred as the best fit for determining the marine geoid as it has the lowest RMSE value between both mission and the maximum degree of 2109^{o} coverage. The finding can assist in development of marine geoid for modelling precise surface elevation.

Keywords: Global geopotential models, marine geoid, gravity anomaly, marine spatial data infrastructure

Corresponding author: amihassan@utm.my

1.0 Introduction

Satellite gravimetry is the latest remote sensing technique presenting a specified global visualisation of the Earth's physical structure for the last two decades. The spatial mass variations and mass transport in the Earth structure could be thoroughly measured and examined from space with the advancement and implementation of CHAMP, GRACE and GOCE missions. Hence, a wide variety of Earth science fields and monitoring systems significant from these observations. Besides, their models can be enhanced and obtained a current comprehension into progressions of the Earth system such as ocean modelling, water cycle, continental hydrology and many more. Thus, future extensive planning has been intended by the Earth science community and space agencies to enable continuous monitoring and observation of mass distribution and transport on a lasting foundation with higher accuracy and better spatial and temporal resolution [1].

The furtherance in satellite gravimetric mission portrays an immense evolution in determining the geoid model with improved accuracy compared to the previous model. A geoid surface is defined as an equipotential surface of the Earth's gravitational field, which coincides beyond any severe factors at the global mean sea surface [2], [3], [4]. Fig. 1 demonstrates a near-accurate illustration of the topographic surface, geoid, ellipsoidal and mean sea surface. The difference between the orthometric height (*H*) and the GPS observed ellipsoidal height (*h*) is called the geoid height or undulation (*N*).

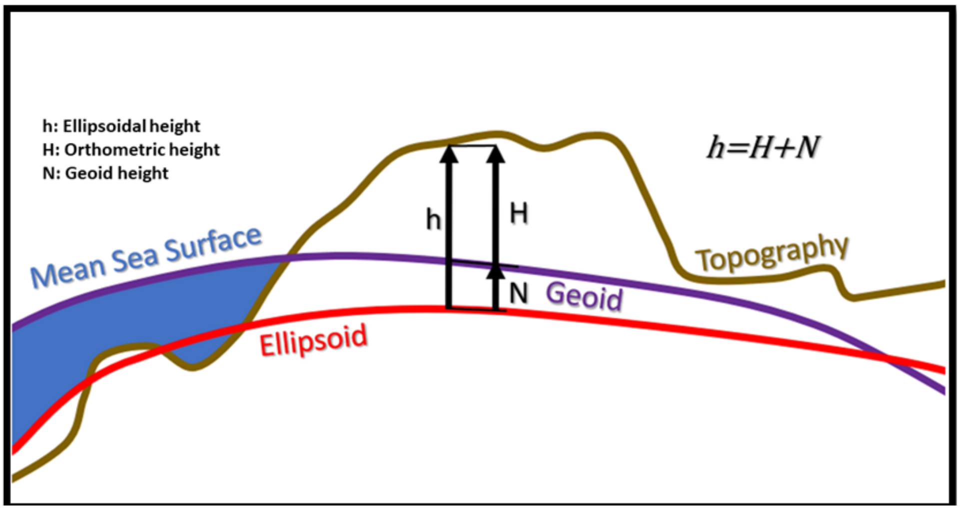

Fig. 1 - Schematic diagram of the topographic surface, geoid, ellipsoid, and mean sea surface [5]

On the contrary, for the marine geoid, the equipotential surface of the gravity adopts the geopotential value from the local mean sea level within the selected marine area. The geoid value for localised areas is indubitably different from the global data as it only concentrated between specific areas. Geoid (and marine geoid) is essential for calculating the precise surface elevations that estimate the mean sea level and depict the average ocean height around the substantial world. Moreover, geoid modelling has progressively increased in significance as one of the vertical datum modernisation elements.

Under the United Nations' Sustainable Development Goals (UN-SDGs) 14, for the sustainable development purposes of conserving and sustainably using the oceans, the information from vertical reference datum, i.e. geoid, is a vital element in developing the uniform database system. Thus, the database system acts as a mechanism to monitor and manage the ocean and marine resources. Besides, the database will also provide timely data recording and updating of information for the stakeholder in coordinating the marine-related activities based on a geographically referenced database infrastructure.

There are 17 goals (see Fig. 2) introduced by UN-SGDs to tackle various global challenges from climate change, global warming, poverty, hunger to inequality with the international partnership cooperation. At present, the International Hydrographic Organization (IHO) and the UN Committee of Experts on Global Geospatial Information Management (UN‐GGIM) and Working Group Marine Geospatial Information (WGMGI) are focused on realizing the Marine Spatial Data Infrastructures (MSDI) for sustainable development and the benefit of the oceans, seas and inland waters, in response to the 2030 Agenda for Sustainable Development by gathering all the information needed [6] and [7].

2.0 Literature Review

In general, the determination of a precise geoid model requires three variation scales, due to the imbalances in the mass distribution in the earth specifically, the long-wavelength component derived from global geopotential model data, the medium wavelength acquired from terrestrial gravity data and the short wavelength from observed terrain model data [8], [9].

Fig. 2 - United Nations on sustainable development goals [7]

The geoid determination from satellite gravimetric data is carried out by combining the short (or medium) wavelength gravity anomalies with the data from the long-wavelength components, which can be obtained from the Global Geopotential Model (after this referred to as GGM) [10]. Afterwards, the data is calculated with modified Stokes' formula formed by Mikhail Sergeevich Molodensky [11].

The GGM represents the 3-dimensional space of Earth's gravitational field approximation in a mathematical function by using spherical harmonic expansions. Moreover, [12] adds that the GGM comprises numerical values for specific parameters, the statistics of the errors and a collection of mathematical expressions, numerical values and algorithms. The GGM represents the global, regional and local data that consists of the satellite-only and combined GGMs. Efforts in developing the GGM using satellite data began in the 1970s with model GEM-1 developed by NASA/Goddard Space Flight Center [13]. Hundreds of GGM are currently available, with free access provided to the scientific community.

[14] and [15] acknowledge that the International Gravity Field Service (IGFS) of the International Association of Geodesy (IAG) has established the International Centre for Global Earth Models (ICGEM) in order to collect and long-term archiving of existing global gravity field models and solutions from dedicated periods. The collected datasets are contributed from different institutions, countries and readily accessible to the public. Moreover, the web portal also performs as a tool for calculating the gravity functionals from the spherical harmonic models based on the specific grids [16]. The user can execute several computations related to gravitational potential (functionals of the field), for instance, gravity anomaly and gravity vector, from the ICGEM website.

The dataset obtained from the ICGEM website is categorised as the satellite-only mission and combined mission. The satellite-only mission depicts the dataset derived from orbit deviation analyses of artificial earth satellites which are satellite gravimetric missions (e.g. CHAMP, GRACE, GOCE and LAGEOS). On the other hand, the combined mission signifies the combination of the dataset from the satellite-only model, satellite gravimeter, satellite altimeter-derived gravity, terrestrial gravimetry, shipborne gravimetry, and airborne gravimetry datasets.

The determination of geoid (in this case, marine geoid) is carried out from the least-squares modification of Stokes' formula, which is commonly called as KTH method developed at the Royal Institute of Technology [17], [18], [19]. KTH method is selected as an approach to determine the geoid model due to the mode of the system used in determining the optimum parameters in geoid computation, which crucial in providing a good accuracy of a geoid model. The geoid height computation is carried out by replacing the gravity anomaly (Δg) and Laplace harmonic gravity anomaly (Δg_n) with observed or computed gravity anomaly (Δg^0) and gravity anomaly derived from Global Geopotential Model (Δg_{GGM}). The indicated data are specified to the area of integration to a spherical cap of the geocentric angle and the upper limit of the GGM to degree *M.* Therefore, as defined by [20] the geoid height (*N*) can be determined based on the Stokes' modification function with additives corrections (best known as the Least Square Modifications of Stoke with Additives Corrections (LSMSA)) and summarised in Eq. (1):

$$N = N^0 + \delta N^{topo}_{comb} + \delta N_{dwc} + \delta N^{a}_{comb} + \delta N^{ell} \qquad (1)$$

where,

N^0 = the estimated geoid,

δN_{comb}^{topo} = the combined topographic correction, which comprises the combination of direct and indirect topographic effects,
δN_{dwc} = the downward continuation effect,
δN_{comb}^{a} = the combined atmospheric correction, which comprises the combination of direct and indirect atmospheric effects and,
δN^{ell} = the ellipsoidal correction for the spherical geoid estimation in Stokes' formula to the ellipsoidal reference surface.

Considering this study is concentrated within the marine area, direct and indirect topographic correction (δN_{comb}^{topo}) has been disregarded. Therefore, in order to compute the estimated geoid (N^0) from Eq. (1), the KTH approach has been employed using the formula from LSMSA which can be expressed in Eq. (2):

$$N^0 = \frac{c}{2\pi}\iint_{\sigma 0} S_L(\psi)\Delta g^0 d\sigma + c\sum_{n=2}^{M} s_n \Delta g_{GGM} \quad (2)$$

where,
c = R/2γ (scale factor),
σ_0 = the spherical cap of the geocentric angle,
S_L = the modified Stokes function, where L is the selected maximum degree of the arbitrary modification parameters S_n,
Δg^0 = the observed or computed gravity anomaly,
M = the degree of the upper limit of the GGM, and
Δg_{GGM} = the GGM-derived gravity anomaly
S_n = the arbitrary modification parameters
n = the order of the upper limit of the GGM

The equations mentioned above (Eq. (1) and Eq. (2)) prove that the derivation of gravity anomaly from the Global Geopotential Model (Δg_{GGM}) has to be provided before the geoid calculation is begun. The GGM dataset is required to contribute the long-wavelength component of gravity anomalies [21]. On account of attaining numerous of the GGM-derived gravity anomaly, the best dataset from either satellite-only or combined-mission needs to be evaluated with the available ground truth data. Correspondingly, one of the premier tasks in determining the geoid is to acquire the most optimum Earth's global gravity field from the GGM. Hence, the KTH method will be utilised for geoid determination and modelling after an appropriate GGM-derived gravity anomaly is determined over the Malaysian region.

This study demonstrates the best GGM-derived gravity anomaly to be utilised in modelling marine geoids within Malaysia seas. Since the ICGEM publishes several GGM, the Earth's potential data generated from the models must be assessed and tested. According to [22] and [23], global evaluation results can be considered a guideline for selecting the appropriate GGM for marine geoid modelling. Thus, the evaluation between the model-derived gravity anomaly dataset regarding existing ground truth terrestrial measurement is the proper fitting to assess the GGM-derived gravity anomaly dataset in a particular area (local or regional level).

3. Methodology

The evaluation of the GGM is a crucial task as it dictated the best optimum long-wavelength data for the next step of determining the localised marine geoid model. Generally, the gravity field measurement is conducted by terrestrial or shipborne surveys that contribute a much higher accuracy compared to the satellite gravimetric technique. Despite that, [24] and [25] identify that some limitations in terms of the distribution of the data and its inconsistencies are included in the techniques (by terrestrial or shipborne surveys). Hence, the satellite gravimetric and other datasets (from spaceborne techniques) are being selected for the gravity measurement since the result gives a reliable and dense gravity data coverage with a better and homogeneous value.

In the interest of determining the Malaysian marine geoid, the selected area grid must cover the Malaysian seas, namely, the Straits of Malacca, South China Sea, Sulu Sea and the Celebes Sea (as shown in Fig. 3) with the geographical data boundary used for all GGM data extraction is between 0° ≤ Latitude ≤ 9°N and 98°E ≤ Longitude ≤ 121°E with a spatial spacing of 0.025.

According to [26], the geoidal heights can be determined from the global distribution of the gravity anomalies. Hence, the gravity anomaly field data based on selected GGMs are extracted within 11 years (2005 until 2015). In addition, 15 models of combined mission and 15 models of the satellite-only mission have been retrieved from the ICGEM web portal to facilitate and accomplish the process.

Subsequently, Table 1 shows the selection of gravity anomaly from the combined satellite missions (GGM) consisting of the mission's detail. The initial of A, G and S in the data column are signified the data from gravimetric satellite (GRACE, GOCE, LAGEOS), altimetry data from satellite altimeter and ground data (e.g., terrestrial, shipborne and airborne measurements).

Meanwhile, for the satellite-only missions, the dataset for gravity anomaly is calculated only from the gravimetric satellites, namely, GRACE, GOCE and LAGEOS, as shown in Tables 1 and 2. Furthermore, the tables also contain the year, maximum degree, and input data for every GGM model. The maximum degree and order information is significant to achieve the higher resolution of spherical harmonics for each model development since the maximum degree of the model expansion corresponds to the spatial resolution (Fig. 4).

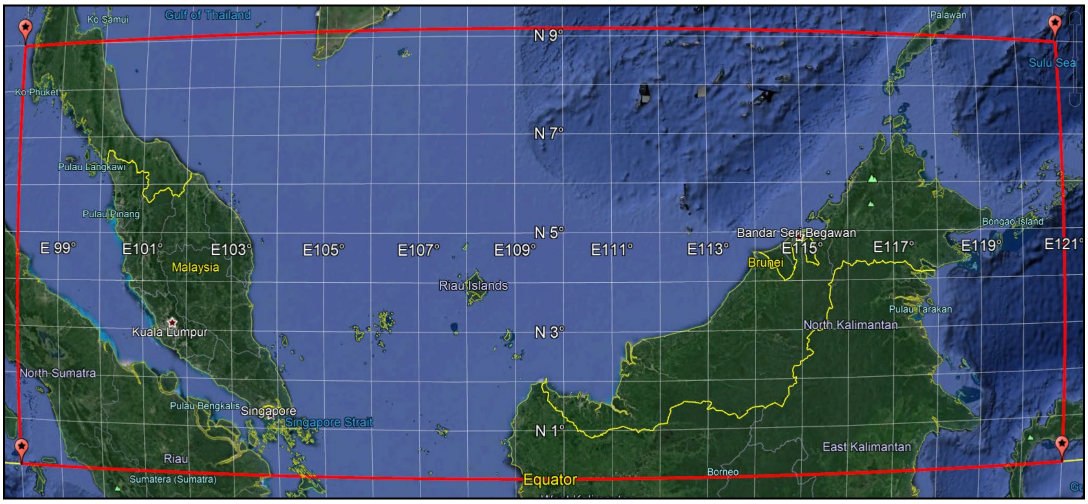

Fig. 3 - Geographical data boundary used in this study covers Malaysian seas

Table 1 - List of Global Geopotential Model for combined mission datasets

No	Model	Maximum Degree	Year	Input Data
1	GOCO05s	280	2015	GOCE, GRACE, Kinematic orbits (8 satellites), SLR (6 satellites)
2	eigen-cg03c	360	2005	A, G, S(CHAMP), S(GRACE)
3	EIGEN-GL04C	360	2006	A, G, S(GRACE), S(LAGEOS)
4	EIGEN-5C	360	2008	A, G, S(GRACE), S(LAGEOS)
5	EGM2008	2190	2008	A, G, S(GRACE)
6	GGM03C	360	2009	A, G, S(GRACE)
7	EIGEN-51C	359	2010	A, G, S(CHAMP), S(GRACE)
8	GIF48	360	2011	A, G, S(GRACE)
9	EIGEN-6C	1420	2011	A, G, S(GOCE), S(GRACE), S(LAGEOS)
10	EIGEN-6C2	1949	2012	A, G, S(GOCE), S(GRACE), S(LAGEOS)
11	GECO	2190	2015	EGM2008, S(GOCE)
12	GAO2012	360	2012	A, G, S(GOCE), S(GRACE)
13	EIGEN-6C3stat	1949	2014	A, G, S(GOCE), S(GRACE), S(LAGEOS)
14	EIGEN-6C4	2190	2014	A, G, S(GOCE), S(GRACE), S(LAGEOS)
15	GGM05C	360	2015	A, G, S(GOCE), S(GRACE)

S=Satellite (CHAMP/GRACE/GOCE/LAGEOS), A=altimetry, G=ground data (e.g., terrestrial, shipborne and airborne measurements)

Table 2 - List of Global Geopotential Model for single mission-only datasets

No	Model	Maximum Degree	Year	Input Data
1	EIGEN-6S2	260	2014	S(GOCE), S(GRACE), S(LAGEOS)
2	GO_CONS_GCF_2_DIR_R3	240	2011	S(GOCE), S(GRACE), S(LAGEOS)
3	GO_CONS_GCF_2_DIR_R4	260	2013	S(GOCE), S(GRACE), S(LAGEOS)
4	GGM05G	240	2015	S(GOCE), S(GRACE)
5	GO_CONS_GCF_2_DIR_R5	300	2014	S(GOCE), S(GRACE), S(LAGEOS)

6	DGM-1S	250	2012	S(GOCE), S(GRACE)
7	GOCO03s	250	2012	S(GOCE), S(GRACE)
8	GO_CONS_GCF_2_TIM_R4	250	2013	S(GOCE)
9	GO_CONS_GCF_2_TIM_R5	280	2014	S(GOCE)
10	GO_CONS_GCF_2_DIR_R1	240	2010	S(GOCE)
11	GO_CONS_GCF_2_TIM_R3	250	2011	S(GOCE)
12	GO_CONS_GCF_2_DIR_R2	240	2011	S(GOCE)
13	GO_CONS_GCF_2_TIM_R2	250	2011	S(GOCE)
14	GO_CONS_GCF_2_SPW_R4	280	2014	S(GOCE)
15	ITG-Goce02	240	2013	S(GOCE)

S=Satellite (CHAMP/GRACE/GOCE/LAGEOS)

Maximum Degree	Number of Coefficients	Resolution ψ_{min}			
		$\psi_{min}(\ell_{max}) \approx \frac{\pi R}{\ell_{max}}$		$\psi_{min}(\ell_{max}) = 4\arcsin\frac{1}{\ell_{max}+1}$	
ℓ_{max}	N	[degree]	[km]	[degree]	[km]
2	9	90.0	10000.000	77.885	8653.876
5	36	36.000	4000.000	38.376	4264.030
10	121	18.000	2000.000	20.864	2318.182
15	256	12.000	1333.333	14.333	1592.587
30	961	6.000	666.667	7.394	821.587
36	1369	5.000	555.556	6.195	688.321
40	1681	4.500	500.000	5.590	621.154
45	2116	4.000	444.444	4.983	553.626
50	2601	3.600	400.000	4.494	499.342
75	5776	2.400	266.667	3.016	335.073
180	32761	1.000	111.111	1.266	140.690
360	130321	0.500	55.556	0.635	70.540
500	251001	0.360	40.000	0.457	50.828
1000	1002001	0.180	20.000	0.229	25.439
2000	4004001	0.090	10.000	0.115	12.726
2190	4800481	0.082	9.132	0.105	11.622

Fig. 4 - Resolution of spherical harmonics [27]

The actual resolution in a specific region depends on the density and quality of the data, including the terrestrial measurements, which are counted in the estimation of the model (Eq. 2). Therefore, the GGM accuracy assessment can be performed by comparing the model to external datasets, e.g., GNSS/terrestrial-derived gravity anomaly. Nevertheless, the outcome is only as good as the external dataset. Thus, the following sections explain the implemented approaches in this study as evaluating and selecting the best fit GGM for geoid determination over Malaysian seas is accomplished. The flowchart of the methodology is illustrated in Fig. 5.

Calculating the GGM-derived gravity anomaly from ICGEM Server within the established geographical data grid

↓

GGM-derived gravity anomaly extraction points based on the airborne-derived gravity anomaly data from along track (200 datapoints are selected at random from each dataset.)

↓

Evaluating the airborne-derived gravity anomaly data with the GGM-derived gravity anomaly at the similar grid size

↓

Analysing the differences between the airborne-derived gravity anomaly and GGM-derived gravity anomaly

Fig. 5 - The flowchart of methodology in this study

3.1 Calculating the GGM-derived Gravity Anomaly from ICGEM Server Within the Established Geographical Data Grid

The global geopotential model accommodates the Newtonian gravitational constant (G) and the Earth's mass information (M), normal gravity on the reference ellipsoid surface (γ), a reference radius (R), fully normalized Stokes' Coefficients for each degree, *n* and order, *m* ($\bar{C}_{nm}$ $\bar{S}_{nm}$) and its respective standard errors ($\sigma\bar{C}_{nm}$ and $\bar{S}_{nm}$). Based on the prior information, the gravity anomaly from global geopotential model can be estimated. Thus, the following Eq. (3) is referred to [5]:

$$\Delta g_{GGM} = \frac{GM}{r^2}\sum\nolimits_{n=2}^{m}\left(\frac{a}{r}\right)^n(-1)\sum\nolimits_{m=0}^{n}\left(\bar{C}_{nm}\cos m\lambda + \bar{S}_{nm}\sin m\lambda\right)\bar{P}_{nm}(\sin\theta) \quad (3)$$

where,

Δg_{GGM}	=	the gravity anomalies from GGM,
GM	=	the mass of the Earth's product and the gravitational constant,
r	=	the radial distance to the computational point,
a	=	the reference ellipsoid's semi-major axis,
$\bar{P}_{nm}$	=	the fully normalised Legendre function, θ,
γ	=	the computation point's geodetic latitude and longitude, and
$\bar{C}_{nm}$ $\bar{S}_{nm}$	=	the fully normalized harmonic coefficients.

Nevertheless, the calculation is managed to be completed from the ICGEM website. The web interface can calculate the gravity field functional, i.e. gravity anomaly from the spherical harmonic representations of the Earth's global gravity field on a preferred grid at will concerning a chosen reference system. [14] describes the server is allowing the user to select several functions freely, according to preference parameter, for example (a) the model of the global gravity field models, (b) the boundaries of the area and the grid interval, (c) the reference system; WGS84 (d) tide system; tide-free (or nontidal) where the direct and indirect effects of the Sun and Moon are removed.

After calculation of gravity anomaly from the GGM is completed, each GGM dataset is extracted by the ICGEM server (http://icgem.gfz-potsdam.de/ICGEM/) in ASCII format and the Generic Mapping Tools (GMT) software [27]. The dataset comprises numerical data and maps view interpretation. All the satellite-only missions are separately restored with the combined missions' data to avoid any confusion. A total of 332481 datasets of gravity anomaly are extracted in this study within the selected area.

3.2 Evaluating the Airborne-Derived Gravity Anomaly Data with the GGM-Derived Gravity Anomaly at The Similar Grid Size

Next, the assessment between the airborne-derived gravity anomaly data and the GGM-derived gravity anomaly data is performed. The following Eq. (4) interprets as the comparison of the residual gravity anomaly from the GGM-derived gravity anomaly and airborne-derived gravity anomaly:

$$\Delta g_{residual} = \Delta g_{GGM} - \Delta g_{airborne} \quad (4)$$

where,

$\Delta g_{residual}$	=	the residual of gravity anomaly,
Δg_{GGM}	=	the GGM-derived gravity anomaly, and
$\Delta g_{airborne}$	=	the airborne-derived gravity anomaly.

The internal statistical for each assessment is computed consists of the minimum value, maximum value, the average, minimum and maximum differences with the airborne-derived gravity data, standard error of the mean, standard deviation and the root mean square. The Root Mean Square Error (RMSE) from Eq. (5) is correspondingly achieved and be utilised as the evaluation for a predicted value and a known value from the standard deviation of the residuals. The equation (Eq. (5)) is the value to accumulate the residuals of both values into a single predictive power measurement. The lowest RMSE dataset will be marked as the highest ranking for both category missions.

$$RMSE = \sqrt{\sum\nolimits_{i=1}^{n}\frac{\left(\Delta g_{GGM} - \Delta g_{airborne}\right)^2}{n}} \quad (5)$$

where,

Δg_{GGM} = the values of GGM-derived gravity anomaly (expected values or unknown results),

$\Delta g_{airborne}$ = the values of GGM-derived gravity anomaly observed values (known results), and

n = number of points.

3.3 Analysing the Differences Between the Airborne-derived Gravity Anomaly and GGM-derived Gravity Anomaly

Once the internal statistical and the RMSE are completely calculated at the later stage, the analysis between both missions is acquired. First, the result can be visualised in a chart to meet better understanding. Next, a thorough investigation is executed to get a better understanding of the result.

The extracted gravity anomaly data from the ICGEM are evaluated with the medium wavelength ground truth data (airborne measurement) due to the lack of short-wavelength components, i.e. shipborne measurement in the Malaysian marine area. The airborne-derived gravity data are obtained courtesy of the Department of Survey and Mapping Malaysia (DSMM) [28] and [29]. The data are the final product from the project under the Marine Geodetic Infrastructures in Malaysian Waters (MAGIC), located in Sabah, Malaysia, from 2014 to 2015. In order to identify the differences between the airborne-derived gravity anomaly and GGM-derived gravity anomaly, 200 data points are selected at random from each dataset.

The following figures (Fig. 5 and Fig. 6) illustrate the airborne tracking points and the model of airborne-derived gravity data from DSMM.

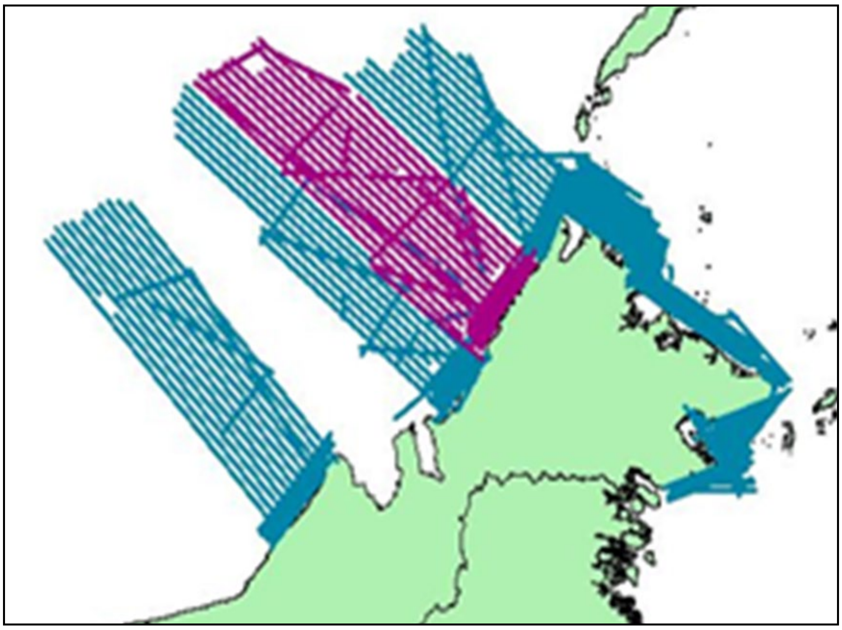

Fig.5 - DSMM's airborne gravity tracking points

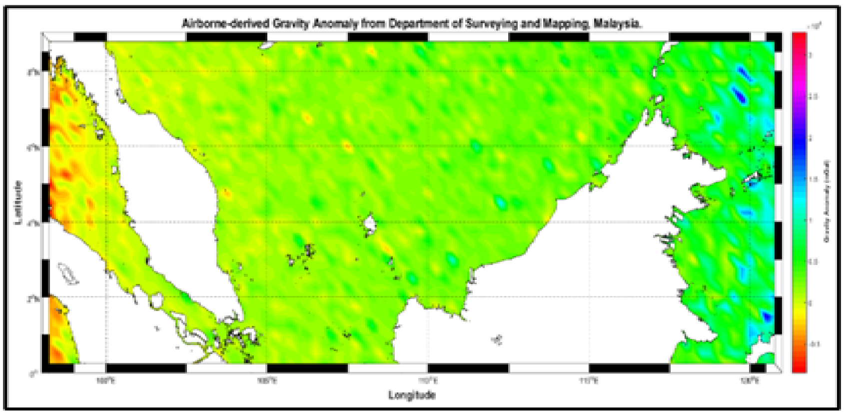

Fig.6 - Airborne-derived gravity data courtesy from DSMM

4. Results and Discussion

ICGEM's data extraction format facilitates the gravity anomaly dataset from every selected mission in terms of spherical harmonic coefficients, the ocean and atmosphere tides. For this study, the combined mission and satellite-only mission are separately analysed to understand data behaviour better.

The value of RMSE from 15 satellite-only missions ranges from 17.43 mGal to 18.83 mGal, with GO_CONS_GCF_2_DIR_R5 marked the lowest RMSE while GO_CONS_ GCF_2_DIR_R2 appears as the highest value of 18.83 mGal. Fig. 7 demonstrates the RMSE values for satellite-only models, and the lowest values of RMSE are portrayed with different colours to differentiate between other results easily.

On the other hand, the RMSE value for combined missions are more prominent as the GECO model signifies the lowest RMSE value among all the models (satellite-only missions included) with 8.44 mGal. On the other hand, the RMSE value range from combined missions is between 8.44 mGal and 20.94 mGal, indicating the GGM05C model has the highest RMSE value (Fig. 8).

It is essential to acknowledge that the GECO model from the combined missions understandably gives the lowest RMSE, considering that the combined mission has the aggregate of numerous datasets, either from gravimetric satellite, altimetry satellite or ground data (terrestrial, shipborne and airborne measurements), a contrast to satellite-only mission dataset. Additionally, the GECO model has the maximum degree of 2190^{o,} verifying that the resolution of spherical harmonics for a model expansion corresponds to the spatial domain.

Besides, the analysis is proven by reviewing specific combined missions' RMSE value that shows a lower value than the result from satellite-only missions. For instance, there are nine missions (GECO, EGM2008, GGM03C, EIGEN-51C, GIF48, EIGEN-6C, EIGEN-6C2, EIGEN-6C3stat and EIGEN-6C4) that are lower than 17.43 mGal (the lowest RMSE value for satellite-only mission: GO_CONS_GCF_2_DIR_R5). Meanwhile, due to the deficiency of the satellite orbit's tracking ground stations and inadequate sampling of global gravity fields' coverage, the satellite-only mission's accuracy and resolutions are lower at a higher degree of coefficients.

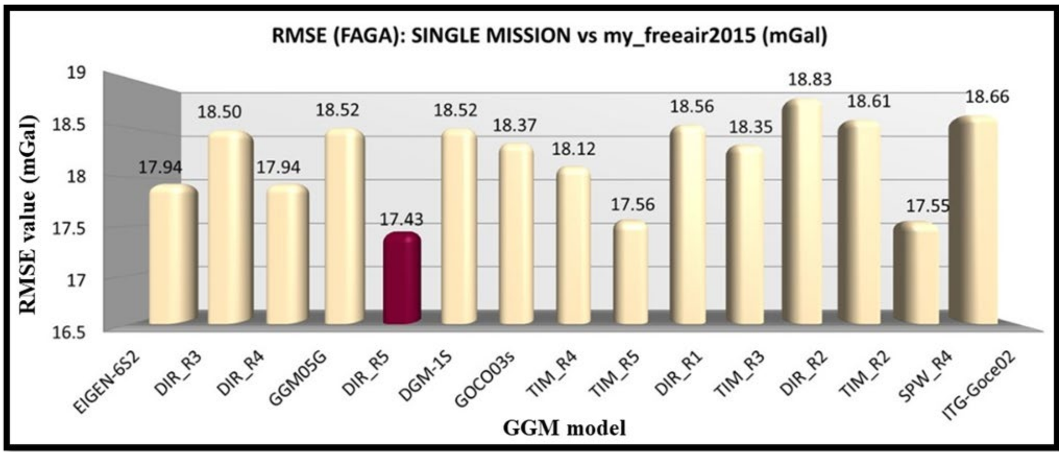

Fig. 7 - RMSE for gravity anomaly from the satellite-only mission with airborne-derived data from DSMM

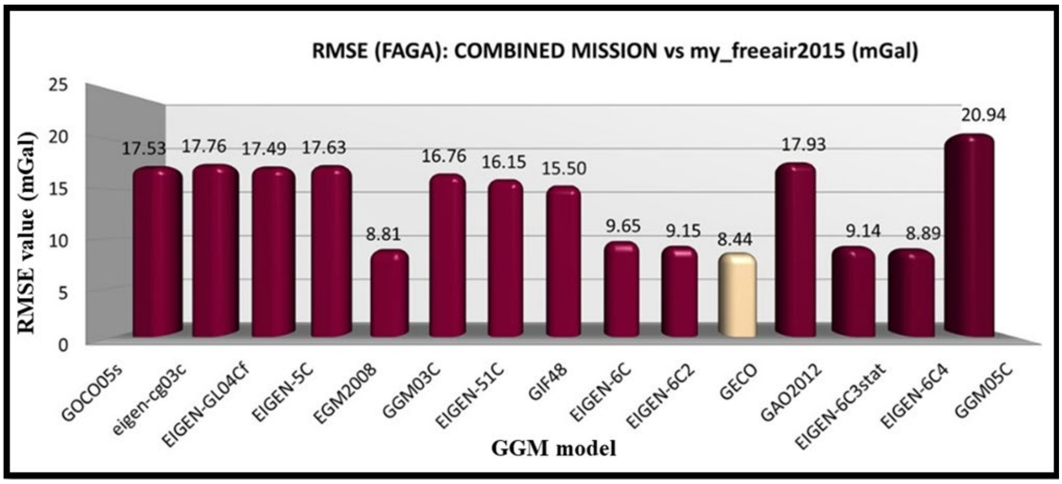

Fig. 8 - RMSE for gravity anomaly from combined satellite mission with airborne-derived data from DSMM

Apart from that, Table 3 presents the internal statistical analysis for GECO, EGM2008 and GGM05C (combined missions) and GO_CONS_GCF_2_DIR_R2, GO_CONS_GCF_2_DIR_R5 and GO_CONS_GCF_2_SPW_R4 for the satellite-only mission, respectively, with the choices of the lowest, second-lowest, and highest of RMSE values have been represented. [22] highlighted that the accuracy of satellite-only GGMs are unconvincing at the higher degree of coefficients because of power decay of the gravitational field with altitude, deficient tracking of satellite orbits utilising ground stations, low precision of non-Earth gravity field stimulated satellite motion, besides insufficient and sparse distribution of global gravity field.

Moreover, Fig. 9 concludes the performances of residual differences (minimum and maximum) between combined and satellite-only missions with the DSSM data. GECO model evinces the smallest maximum and minimum differences of 73.50 mGal between other models. The result shows a higher correlation between the combined mission datasets (GECO model and EGM08) with the airborne-derived gravity anomaly as aforementioned before.

From both statistical analyses, the model from combined mission GGM, GECO, is the best fit to represent the long-wavelength component to determine the localised marine geoid. Notwithstanding, the GGM evaluation only implied the best result for a particular area since the coverage, quality and accuracy of the dataset within the study area are vary from one region to another.

Table 3 - The internal statistical analysis for GECO, EGM2008 and GGM05C (Unit: mGal)

	GECO	EGM2008	GGM05C	DIR_R5	SPW_R4	DIR_R2
Min	-106.04	-108.36	-42.22	-55.14	-54.25	-56.43
Max	256.86	258.01	137.73	147.20	148.28	159.22
Average	23.47	23.47	23.57	23.71	23.70	23.75
Std Error of The Mean	0.05	0.051	0.03	0.04	0.04	0.04
Std Dev	28.03	28.32	20.73	22.83	22.49	22.77
RMS	36.56	36.78	31.39	32.91	32.68	32.91
Min Diff (With DSSM)	-240.06	-238.65	-358.73	-344.90	-342.74	-345.10
Max Diff (With DSSM)	73.50	81.21	98.24	112.91	113.01	105.43

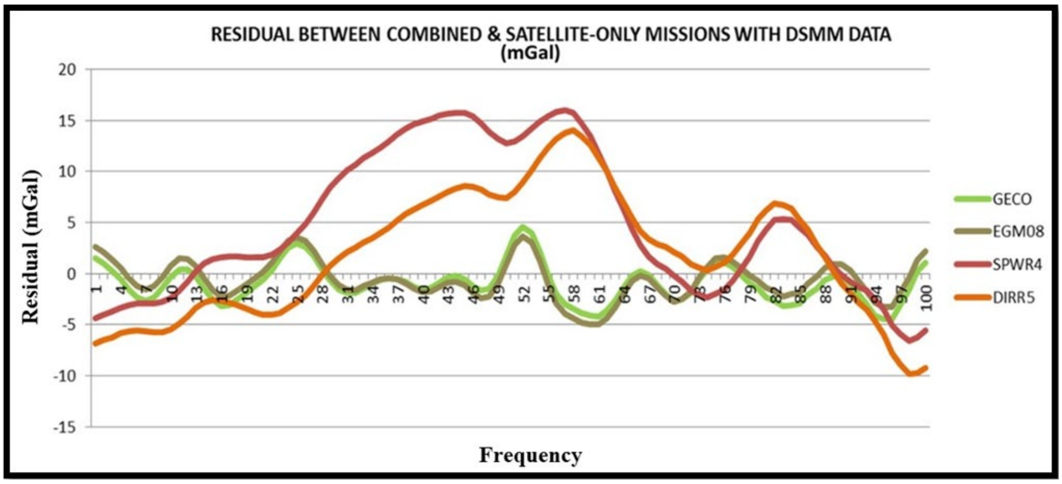

Fig. 9 - Residual differences between the combined and satellite-only missions with DSSM data

5. Conclusion

The assessment of the GGM with ground truth data is essential to find the best fit of the long-wavelength gravimetric mission for determining the localised marine geoid. Fifteen models of combined mission and 15 models of the satellite-only mission have been employed to facilitate and accomplish this assessment. As a result, the combined mission dataset of GECO is established as the best fit for determining the marine geoid for the Malaysian seas. The GECO mission comprises several datasets from the gravimetric satellite, altimetry satellite, and ground data, either from terrestrial, shipborne or airborne measurements. Eventually, the result represents the characteristics and data features of the global geopotential models correlated within the particular area that may not be compatible with other areas. Besides that, the degree and order of the model depict the essential element to achieve a better resolution geoid, given that the GECO model has the highest maximum degree and the lowest RMSE value compared to the others.

Nevertheless, if the Marine Geoid for Malaysia is to be based on satellite-only GGM, GO_CONS_GCF_2_DIR_R5 could be a suitable candidate.

Based on this result, it is shown that the selection of the GGM model will have an impact on the development of gravimetric geoid modelling. However, the presented investigation only revolved between satellite-derived gravity anomaly, specifically, the satellite-only and combined missions, signifying only the long and medium wavelength assessment. Therefore, it would be helpful to extend this investigation to evaluate different spherical harmonic degrees and orders of the global geopotential model for better resolution outcomes.

Concluding to this assessment, it is highly recommended that the evaluation of GGM with airborne gravity data can be contributed towards the determination of marine geoid with the enhancement of the latest technology, for instance, the application of satellite altimeter and the existing gravimetric satellite to provide higher resolution and denser data potentially. Addiction to that, the information from marine geoid enacts as a role to the development of Marine Spatial Data Infrastructures (MSDI) for the sustainable development and the benefit of the oceans, outlined by UN SDG 14.

Acknowledgements

The authors would like to thank the Department of Survey and Mapping Malaysia (DSMM) for the airborne gravity data under the Marine Geodetic Infrastructures in Malaysian Waters (MAGIC) Project over marine areas in Sabah year 2014 and 2015. In addition, special thanks are due to the International Gravity Field Service (IGFS) of the International Association of Geodesy (IAG) for providing the global gravity data on the International Centre for Global Earth Models (ICGEM) website. This project is funded by the Ministry of Higher Education (MOHE) under the Fundamental Research Grant Scheme (FRGS) Fund, Reference Code: FRGS/1/2020/WAB07/UTM/02/3 (UTM Vote Number: R.J130000.7852.5F304).

References

[1] Gruber, T., Eicker, A., & Flechtner, F. (2021). Remote sensing by satellite gravimetry. Remote Sensing. https://www.mdpi.com/journal/remotesensing/special issues/satellite gravimetry)
[2] Torge, W., & Müller, J. (2012). Geodesy. Walter de Gruyter.
[3] Denker, H. (2013). Regional gravity field modelling: Theory and practical results. In Xu G. (eds), Sciences of Geodesy-II, Springer.
[4] Sulaiman, S. A. (2016). Gravimetric geoid model. PhD Thesis. Universiti Teknologi Mara, Malaysia.
[5] Heiskanen, W. A., & Moritz, H. (1967). Physical Geodesy. W. H. Freeman and Company.
[6] International Hydrographic Organization (2019). Monthly Meeting Report. https://www.iho.int/iho_pubs/IHO-bulletin/briefmeetingreports/2019/March_2019.pdf
[7] United Nations (2015). Transforming our world: The 2030 agenda for sustainable development. United Nation Sustainable Development Summit 2015, New York.
[8] Heliani, L. S. (2003). Determination of Indonesian geoid from combination of surface gravity, satellite altimetry and global terrain model data. Kyoto University.
[9] Hofmann, B., & Moritz, W. H. (2005). Physical Geodesy. Springer Wein.
[10] Sjoberg, L. E. (2003). A computational scheme to model the geoid by the modified Stokes formula without gravity reductions. Journal of Geodesy, 77(7-8), 423-432.
[11] Molodensky, M. S., Eremeev, V., & Yurkina, M. (1962). Methods for study of the external gravitational field and figure of the Earth. Israel Program for Scientific Translations, Jerusalem.
[12] Rapp R. H. (1998). Past and future developments in geopotential modeling. In Forsberg R., Feissel M., & Dietrich R. (eds) Geodesy on the Move. International Association of Geodesy Symposia, Springer.
[13] Pavlis N. K. (2013). Global gravitational models. In Sansò F., & Sideris M. (eds) Geoid Determination: Lecture Notes in Earth System Sciences, Springer.
[14] Ince, E. S., Barthelmes, F., Reißland, S., Elger, K., Förste, C., Flechtner, F., & Schuh, H. (2019). ICGEM – 15 years of successful collection and distribution of global gravitational models, associated services and future plans. Earth System Science Data, 11, 647-674.
[15] Barthelmes, F. (2014). Global models. In Grafarend E. (eds) Encyclopedia of Geodesy. Encyclopedia of Earth Sciences Series, Springer.
[16] Drewes, H., Kuglitsch, F., Adám, J., & Rózsa, S. (2016). The geodesists handbook. Journal of Geodesy, 90(10), 907-1205.
[17] Ulotu, P. E. (2009). Geoid model of Tanzania from sparse and varying gravity data density by the KTH Method. PhD Thesis, Royal Institute of Technology (KTH), Sweden.
[18] Abbak, R. A., Erol, B., & Ustun, A. (2012). Comparison of the KTH and remove-compute-restore techniques to geoid modelling in a mountainous area. Computers and Geosciences, 48, 31-40.

[19] Yildiz, H., Forsberg, R., Ågren, J., Tscherning, C., & Sjöberg, L. E. (2012). Comparison of remove-compute-restore and least squares modification of Stokes' formula techniques to quasi-geoid determination over the Auvergne test area. Journal of Geodetic Science, 2(1), 53-64.
[20] Pa'suya, M. F., Yusof, N. N. M., Din, A. H. M., Othman, A. H., Som, Z. A. A., Amin, Z. M., Aziz, M. A. C., & Samad, M. A. A. (2018). Gravimetric geoid modelling in the northern region of peninsular Malaysia (NGM17) using KTH method. IOP Conference Series: Earth and Environmental Science, 169, 012089.
[21] Yazid, N. M., Din, A. H. M., Omar, K. M., Som, Z. A. M., Omar, A. H., Yahaya, N. A. Z., & Tugi, A. (2016). Marine geoid undulation assessment over South China Sea using global geopotential models and airborne gravity data. International Archives of the Photogrammetry, Remote Sensing and Spatial Information Sciences, XLII-4(W1), 253-263.
[22] Kiamehr, R. (2006). Precise gravimetric geoid model for Iran based on GRACE and SRTM data and the least-squares modification of Stokes' formula with some geodynamic interpretations. Phd Thesis, Royal Institute of Technology (KTH), Sweden.
[23] Tugi, A, Din, A. H. M., Omar, K. M., Mardi, A. S., Som, Z. A. M., Omar, A. H., Yahaya, N. A. Z., & Yazid, N. M. (2016). Gravity anomaly assessment using GGMs and airborne gravity data towards Bathymetry estimation. International Archives of the Photogrammetry, Remote Sensing and Spatial Information Sciences, XLII-4(W1), 287-297.
[24] Xu, C., Weigelt, M., Sideris, M. G., & Sneeuw, N. (2007). Spaceborne gravimetry and gravity field recovery. Canadian Aeronautics and Space Journal, 53(3-4), 65–75.
[25] Stokes, G. G. (1849). On the variation of gravity at the surface of the earth. Transactions of the Cambridge Philosophical Society, VIIII, 672–695.
[26] Barthelmes, F., & Köhler, W. (2015). Tutorial on height and gravity. EUREF Symposium 2015, Leipzig, Germany.
[27] Wessel, P., Smith, W. H., Scharroo, R., Luis, J., & Wobbe, F. (2013). Generic mapping tools: Improved version released. Eos, Transactions, American Geophysical Union, 94, 409-410.
[28] JUPEM (2014). The conduct of airborne gravity and magnetic survey over selected area near the international maritime boundary offshore of Sabah and Sarawak, Phase 1 (2014), Contract JUPEM-T03/2013. Final Report. Bahagian Ukur Geodetik.
[29] JUPEM (2015). The Conduct of airborne gravity and magnetic survey over selected area near the international maritime boundary offshore of Sabah and Sarawak, Phase II (2015), Contract JUPEM-T-24/204. Final Report. Bahagian Ukur Geodetik.